Sonar Aided Navigation and Control of Small UUVs

Đula Nađ[1], Nikola Mišković[1], Vladimir Djapic[2] and Zoran Vukić[1]

***Abstract*— This paper addresses the problem of guiding a simple unmanned underwater vehicle (UUV) from a more capable, sonar equipped, platform, preferably an autonomous underwater or surface vessel (AxV). One application of this concept, considered in this article, is autonomous mine neutralization and disposal. First, a sonar equipped AxV acquires a possible target in the sonar image. Once the target location is known, an expendable UUV is released. The UUV position is determined from sonar imagery onboard the AxV. This minimal information is sent to the UUV via acoustic link so that it can converge towards the desired target. With this approach, complex and expensive sensors are removed from the expendable vehicle, which now becomes a simple actuation system that carries the neutralization payload, and this in turn greatly increases cost efficiency. Although we review the concept in the domain of mine countermeasures (MCM) it is applicable to other problems where navigation aiding between platforms is beneficial. This paper focuses on preliminary results obtained in numerous pool and field experiments during different phases of system development.**

I. Introduction

Most modern AxVs provide an aided inertial system (AINS) as their navigation solution. AINS systems are based around inertial measurement unit (IMU) aided by a Doppler velocity log (DVL), depth sensor and underwater or global positioning system [10]. Aiding sensors are needed to reduce the drift rate or periodically reset position estimates. Modern INS systems are specified as being capable of heading drift rates of less than 0.01 deg/hr [2]. High accuracy comes with higher cost, which is acceptable for non-expendable AxVs, but is not desired for expendable (one-shot) UUVs, which are taken into consideration in this paper. Although the cost factor eliminates the complete AINS solution from the equation, a basic sensor suite, e.g. compass and pressure sensor, remains as a minimal requirement.

The main objective of the proposed system is for the UUV to follow a 3D path, therefore the basic sensor suite needs to be expanded with position measurements. Higher frequency long baseline (LBL) systems can offer sub-centimeter precision and update rates up to 10 Hz [7]. However, precise mooring of LBL transponders is required. Alternatively, GPS intelligent buoy (GIB) systems offer adequate performance without the need for transponders to be precisely moored on the sea-floor [1]. On the other hand, transponder deployment and recovery is still necessary. This issue can be resolved by using an ultra short baseline (USBL) system on a support platform. The downside of a USBL system is performance degradation with higher elevation angle, especially noticeable in shallow waters.

This paper presents our ongoing research of using a multibeam imaging sonar instead of LBL/USBL systems for the purpose of UUV navigation aiding. From the sonar image, UUV range and bearing relative to the sonar head can be measured, similarly to a USBL system. However, higher multibeam resolution offers better precision in comparison to USBL measurements. The downside is that the UUV has to remain in the sonar beam. This can be solved by mounting a sonar on a pan and tilt system. With our approach, a mine neutralization UUV can be small and inexpensive with a basic sensor suite and an acoustic receiver for receiving measurement updates obtained from the sonar image. In addition, the paper advocates the potential of using collaborative autonomous vehicles in MCM scenarios. In the envisioned concept of operations, an AxV reacquires a mine-looking target using its imaging sonar. Immediately following, the AxV guides a low-cost neutralization UUV carrying a payload to neutralize the target. Collaboration between the highly capable AxV and the low-cost, hence less capable, mine neutralization UUV is viewed as an interesting research subject in the field of mine reacquisition and neutralization since it can potentially drastically reduce the overall MCM mission timeline.

A. System description

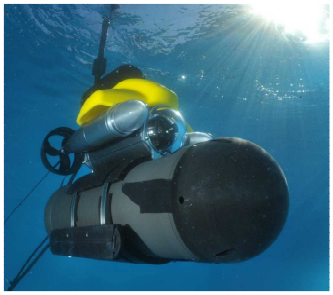

Fig. 1. The UUV developed for the MCM mission.

1) The automatic UUV: The automatic UUV shown in Fig. 1 is a modification of the VideoRay Pro IV submersible. An additional hull attached to the bottom of the remotely operated vehicle (ROV) is equipped with a PC board, batteries,

The work was carried out in the framework of a Coordination and Support Action type of project supported by European Commission under the Seventh Framework Programme "CURE – Developing Croatian Underwater Robotics Research Potential" SP-4 Capacities (call FP7–REGPOT–2008–1) under Grant Agreement Number: 229553.

This work was also supported by North Atlantic Treaty Organisation via NURC's CPOW - Consolidated Programme of Work.

[1] University of Zagreb, Faculty of Electrical Engineering and Computing, LabUST - Laboratory for Underwater Systems and Technologies Unska 3, Zagreb, Croatia

[2]NATO Undersea Research Centre (NURC), Viale S. Bartolomeo 400, La Spezia 19126, Italy

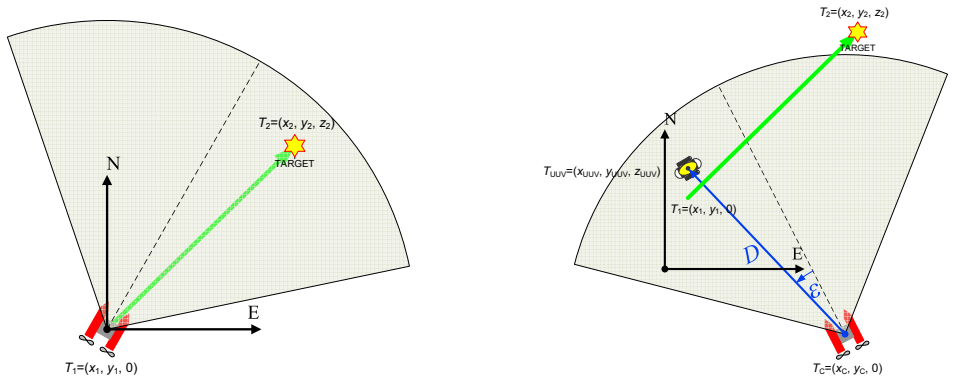

(a) Before deployment (b) After deployment

Fig. 2. Deployment scenario

additional electronic components and an acoustic receiver. In the current version, both an acoustic link as well as a thin cable connected to the UUV can be used for communication. It is equipped with two horizontal thrusters and one vertical thruster, making it an underactuated system fully controllable in surge, yaw and heave degrees of freedom. The main task of the UUV is to converge towards the desired line (connecting the initial UUV position and target position) once deployed.

2) The forward looking multibeam sonar: The BlueView P900 was used as the multibeam sonar. During the initial testing phase the sonar was fixed, while in the future it will be mounted on the mobile AxV. Using a multibeam sonar for navigation aiding gave good results. It was noticed that robustness and accuracy of position estimation was directly dependent on image processing. Errors such as misalignment and image calibration can be removed with careful setup. However, more research time needs to be invested in increasing the robustness of UUV detection within the sonar image.

II. Mission Scenario

The mission includes two vessels:

1) a small, inexpensive, and expendable UUV with the least sensors possible (depth sensor, compass and an acoustic receiver) – UUV;
2) a remote observing and sensing surface platform which guides the underwater vehicle to the target using sonar imagery – AxV.

Imagine that mine detection was performed by the AxV on a certain region and that one mine like object was identified. Once the target identification is successful, the AxV is ordered to neutralize the target. Target coordinates, $T_2 = (x_2, y_2, z_2)$ and current AxV position, $T_1 = (x_1, y_1, z_1)$, are recorded. These coordinates define a 3D line between the AxV and the target, as shown in Fig. 2(a). Note the assumption that the target depth is known.

The AxV carries an armed expendable UUV within its payload. On the neutralization order, the UUV is launched. Prior to the launch, the AxV notifies the UUV about the target position. From this point on the algorithm inside the UUV starts following the path set by points T_1 and T_2. Upon detection of the UUV in the sonar image the AxV starts sending position updates to the UUV, as in Fig. 2(b). Algorithms are executed separately onboard each vehicle, as shown in diagram of Fig. 3.

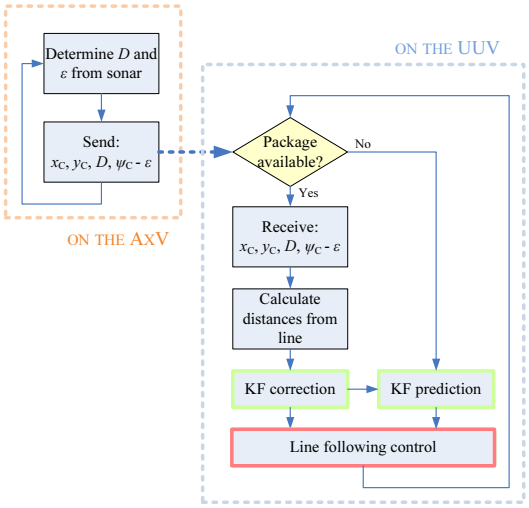

Fig. 3. Algorithms executed onboard the AxV and the UUV.

Onboard the AxV, range D and bearing ε of the UUV with respect to the sonar head are determined from the sonar image (see Fig. 2(b)). Then the AxV sends the coordinates of the vehicle x_C and y_C, range D and $\psi_C + \epsilon$ where ψ_C is the heading of the AxV at a rate dependent on the communication link quality. The amount of data that is sent to the UUV should be minimized for the acoustic communications mode of operation.

Simultaneously, onboard the UUV, the following algorithm is executed, with a constant update rate of 10 Hz. If a data packet from the AxV is available, D, x_C, y_C and $\psi_C + \epsilon$ are received. Locating the UUV in the sonar image does not provide enough information for the localization of the UUV. By adding the depth z_{UUV} (available at the UUV), (1) and (2) are used to calculate the measured position. Usually a measurement will be delayed due to transmission. When the delay is longer than the Kalman Filter update period the correction is applied to the past prediction step. A new

prediction is performed from the past to the current time step in order to calculate the corrected position estimate. Based on this position, horizontal and vertical distances to the desired line are estimated:

$$x_{UUV} = x_c + \cos(\psi_c + \varepsilon)\sqrt{D^2 - z_{UUV}^2}, \quad (1)$$

$$y_{UUV} = y_c + \sin(\psi_c + \varepsilon)\sqrt{D^2 - z_{UUV}^2}. \quad (2)$$

Since the update rate of measurements received through the acoustic link is much lower, a Kalman filter for state estimation (when the measurement are not available) has been designed (see Section III-C).

Remarks. The main advantages of the proposed system configuration are as follows:

1) This approach utilizes one way communication between the UUV and the AxV. Any other approach would require the UUV to send its depth to the AxV.
2) The proposed Kalman filtering enables UUV navigation in the cases where measurements are not available.
3) The multibeam sonar mounted on the AxV need not have the target and the UUV in the field of view at all times, but only the UUV. If the target is in the field of view, corrected target position can optionally be sent to the UUV.
4) If the AxV drifts due to currents, the UUV will not drift with it but it will stay and the line which has been determined initially.

III. Modeling and Control

A. Line-following mathematical model

Let us define the 3D oriented line ℓ with two points, T_1 and T_2. The 3D line-following problem can then be separated into two 2D line-following problems:

- the horizontal line ℓ_H defined with T_1 and angle Γ in the N-D plane, Fig. 4(a), and
- the vertical line ℓ_V defined with T_1 and angle χ in the N-E plane, Fig. 4(b).

The following mathematical models are derived for the observed UUV specific thruster allocation. Details of the model formulation can be found in [12].

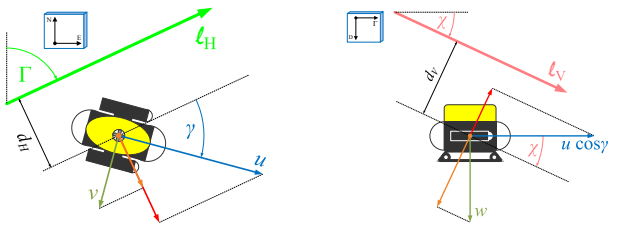

Fig. 4. The 3D line-following decomposition: (a) ℓ_H following model and (b) ℓ_V following model (UUV is assumed aligned with ℓ_H).

1) The ℓ_H line-following model: The model for following of the line ℓ_H, shown in Fig. 4(a), can be described by:

$$\dot{d}_H = u\sin\gamma + v\cos\gamma + \xi_H, \quad (3)$$

$$\dot{\gamma} = r \quad (4)$$

$$\dot{r} = -\frac{\beta(r)}{\alpha_r}r + \frac{k_{ru}}{\alpha_r}ru + \frac{1}{\alpha_r}N. \quad (5)$$

The vehicle's approach towards the line is achieved by controlling the attack angle $\gamma = \psi - \Gamma$. Surge speed is needed for d_H to converge to zero. We assume a constant surge force X_{ref}. The terms $v\cos\gamma$ and ξ_H can be considered as external disturbances which have to be compensated for. The yaw dynamics are given by Eq. (5); where α_r is yaw inertia and $\beta(r)$ is yaw drag which is assumed to be purely constant or linear. During the experiments, the UUV exhibited pronounced coupled dynamics between yaw rate and surge speed. In order to compensate for this, the coupling effect is included in yaw dynamics.

2) The ℓ_V line-following model: The mathematical model for following the line ℓ_V, shown in Fig. 4(b), is described by:

$$\dot{d}_V = w\cos\chi - u\cos\gamma\sin\chi + \xi_V, \quad (6)$$

$$\dot{w} = -\frac{\beta(w)}{\alpha_w}w + \frac{1}{\alpha_w}(Z + W - B). \quad (7)$$

The distance d_V changes due to surge u and heave w as shown in Eq. (6). External disturbances and unmodelled dynamics are described by ξ_V. Heave dynamics are given by Eq. (7) with B being buoyancy and W weight of the UUV.

B. Control design

1) The ℓ_H line-following controller: The line-following controllers used in this work were introduced in [3]. The horizontal line-following controller consists of an inner yaw rate controller and outer line-following controller. Linearization of the kinematic model, i.e., $\sin\gamma \approx \gamma$, as well as direct actuator control are assumed. The yaw rate controller is augmented with a term $k_{ru}ru$ which compensates for the coupling effect in the yaw dynamic model, Eq. (5). Surge speed u is not measured, therefore we assume that $u \sim X_{ref}$. Here X_{ref} is the commanded surge thrust. The feed-forward term $k_{ru}X_{ref}r_{ref}$ is introduced, assuming that $r_{ref} \approx r$:

$$N_{ref} = K_{Ir}\int_0^t (r_{ref} - r)\,dt - [K_{Pr} - \beta(r)]r + \tilde{k}_{ru}r_{ref}X_{ref} \quad (8)$$

The outer control loop is of the PD (proportional–derivative) type, given by

$$r_{ref} = K_{Ph}(d_{H,ref} - d_H) + K_{Dh}\frac{d}{dt}(d_{H,ref} - d_H), \quad (9)$$

where $d_{H,ref} = 0$, i.e. convergence to the line is required.

2) The ℓ_V line-following controller: The vertical line-following controller is derived in a similar manner. The controller algorithm is given in Eq. (10) where the output is the desired heave force Z_{ref}:

$$Z_{ref} = K_{Iv} \int_0^t (d_{V,ref} - d_V)\, dt - K_{Pv} d_V - \frac{d}{dt} d_V. \quad (10)$$

The presented controllers depend on the dynamic parameters of the UUV. Since different payloads can be attached to the UUV, different dynamics can be expected, therefore the identification should always be performed before the mission starts (right after deployment). The UUV identification (in yaw and heave degree of freedom) is performed by using the self-oscillation identification method [11], which has proven to be quick and applicable in in-field conditions.

C. UUV navigation

UUV navigation uses the Extended Kalman Filter (EKF) for state estimation. The mathematical model described in Section III-A is used in the estimator. Outputs of the estimator are horizontal and vertical distances from the line. Additionally, compass and pressure sensor information is filtered as well. EKF initialization is done after the UUV deployment. Based on points T_1 and T_2, from Section II, the line-following model is initialized.

After the complete initialization, line-following is engaged. Estimator outputs are used as feedback values for the controller. Estimations are output at 10 Hz. Measurements received from the AxV limit the drift of the estimator. The frequency of the received measurements varies due to the communication channel, but has a minimum value of 0.5 Hz.

IV. Sonar image processing

Sonar data processing is a crucial part of the system. Line-following accuracy is directly related to the accuracy of the position extracted from the sonar image. This can present a problem in a cluttered environment with many strong reflections.

Imaging sonars have been used in navigation aiding before, see [6], [5], [13] and references therein. These applications mainly include using the sonar for the purpose of feature extraction in order to navigate the vessel carrying the sonar. In our case, the extracted feature is the vessel itself, and the task is to aid its navigation. Therefore, only one feature is tracked and *a priori* information about it is at our disposal, i.e., a smaller part of the image data needs to be processed. However, in this case, the tracked feature is small and moving away from the sonar, which presents an additional challenge.

Image processing is separated into several steps, as shown in Fig. 5. Although sonar data is more naturally represented in polar coordinates (using range r and bearing ϕ), in this application the data is analyzed in the Cartesian coordinate system (x–y). The reason for this is that most existing image analysis tools work on x–y images. During the initialization

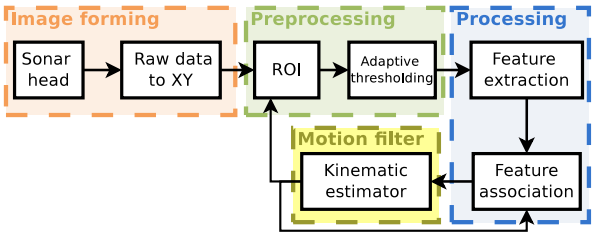

Fig. 5. The sonar image processing chain.

phase, the extended region around the sonar is searched for a potential UUV signature. Once detected, the tracking estimator is initialized. The UUV range and bearing in the sonar image, as well as, the absolute position of the sonar head are then reported to the UUV navigation system.

In the following iterations, the region of interest (ROI) is selected based on the estimated UUV position in the sonar image. Limiting the search region improves performance as well as limits the amount of false detections. Adaptive thresholding is performed in the ROI to detect the strongest reflections. The data is grouped into clusters and small clusters are removed. The remaining features are then filtered using the "nearest neighbour" filter [8]. In other words, the feature closest to the estimated position is selected as the new update of the model.

Feature association is required since the UUV cannot be directly recognized in the sonar image. Therefore, it can only be assumed that one of the features is the UUV. Static features are more likely to be misclassified as the UUV if each image is observed separately. This is why target movement estimation is applied. This approach requires a motion model to be defined. As the first step, a standard 2D kinematic model which assumes linear UUV motion with constant speed is proposed:

$$x(k+1) = x(k) + T_s\, U(k)\, cos\psi(k) \quad (11)$$
$$y(k+1) = y(k) + T_s\, U(k)\, sin\psi(k) \quad (12)$$
$$U(k+1) = U(k) + \xi_U(k) \quad (13)$$
$$\psi(k+1) = \psi(k) + \xi_\psi(k) \quad (14)$$

where x and y are detected UUV coordinates, U is UUV forward speed, ψ is UUV course and ξ_U and ξ_ψ represent process noise and unmodelled dynamics. Note that this model is applicable only to a static sonar platform. The 3D motion in world coordinates cannot be estimated since UUV depth cannot be reliably detected – the reason for this lies in the fact that this system configuration does not have return communication from the UUV (as it was elaborated in Section I). In future work, the position estimation scheme will use a Kalman filter for model propagation. Once performance with this model is evaluated, a more complex model that incorporates platform movement will be implemented. In addition to that, more sophisticated (and more computationally demanding) algorithms for target tracking (such as [9], [4], [8]) will be tested and compared

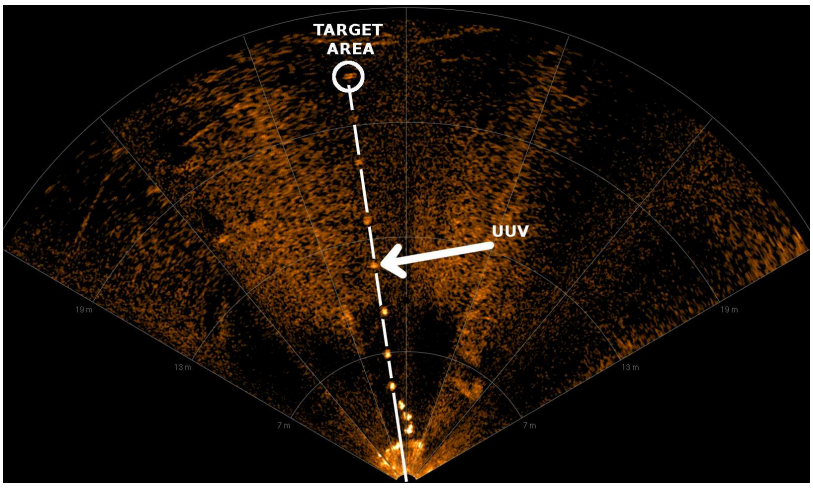

Fig. 6. Multibeam sonar image with UUV traces in time as a result of field experiments.

to the current algorithm. However, our current focus is on providing a computationally inexpensive method for sonar image processing that can be embedded into less powerful hardware on the AxV.

Initial experiments were focused around the UUV navigation and control. Therefore, the feature association was simplified. This proved to be adequate for testing in real-life conditions, up to 35 m sonar range, where the vehicle moves with slow constant speed. Most experiments during the initial phase were conducted in medium to low cluttered environments. Performance in a highly cluttered environment remains to be researched. The authors expect degradation of performance, but implementing the whole chain in Fig. 5 is expected to partially alleviate the problem.

V. Results

Several experiment phases were carried out as part of initial development and testing:

- In July 2010, image processing and line-following was implemented in NATO Undersea Research Centre, La Spezia, Italy (example result shown in Fig. 6);
- At the end of September 2010, the autonomy module was mounted on the vehicle, and pool testing was performed during the "Breaking the Surface 2011" workshop in Murter, Croatia (result example shown in Fig. 7);
- At the end of November 2010, acoustic communication was implemented and guidance over the acoustic link was tested in field conditions in NATO Undersea Research Centre, La Spezia, Italy (result example shown in Fig. 8).

The first experiments were performed with a stock VideoRay Pro 3 vehicle. The testing proved the concept to be feasible. Simple image processing was used to extract vehicle range and bearing. Control and navigation, implemented in LabView, was running on a separate computer. The UUV movement is shown in Fig. 6, showing 12 combined frames from the sonar data. The video can be downloaded directly at `http://lapost.fer.hr/media/movies/multibeam_sonar.mpeg`. During this experiment, thruster commands were sent to the vehicle through a tether.

During the September testing, the main autonomy module functionality was tested. Due to the limited pool depth, only horizontal performance was tested. Horizontal distance convergence is shown in Fig. 7. Initial position of the UUV was 2 m away from the desired line with the UUV almost aligned with the line. It can be observed that the heading,ψ, and horizontal distance, d_H, are converging which indicates that the control system is functional even with the attached autonomy module. During these experiments strong coupling between surge and yaw was observed, which resulted in the modified control algorithm given by Eq. 8. The conclusion was that the coupling is due to the size and the torpedo shape of the autonomy module.

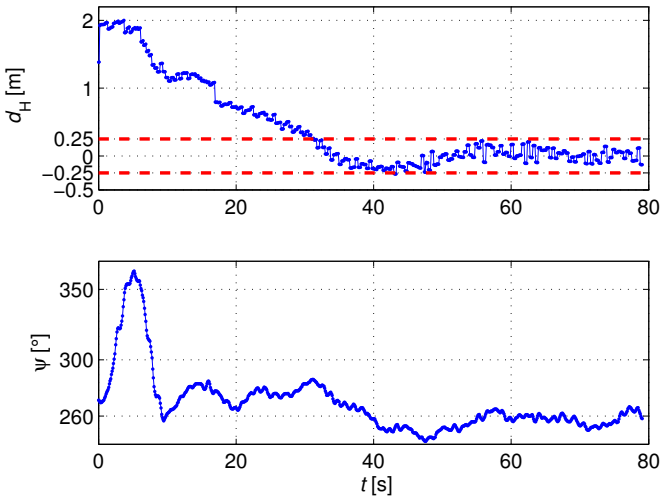

Fig. 7. Performance of the UUV during experimental trials – horizontal distance d_H and UUV's heading ψ.

The first experiments with the acoustic link were performed in late November 2010. The UUV control algorithms were all performed inside the autonomy module. Position

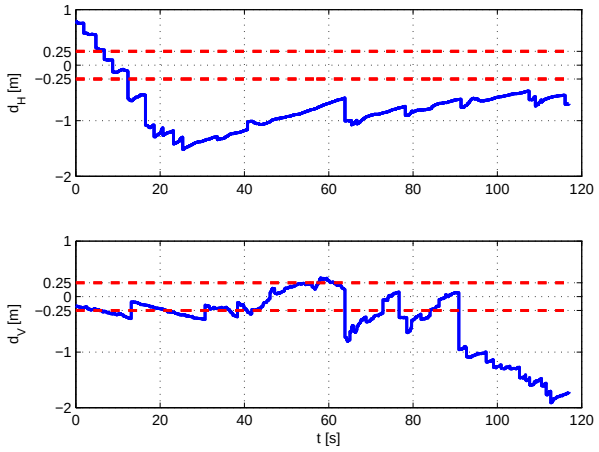

Fig. 8. Performance of the UUV during the acoustic link testing.

updates were sent through the acoustic link every second. Experimental data shown in Fig. 8 display the horizontal and vertical distance from the line. Horizontal distance converges to 0.5 m from the line, while vertical distance starts increasing after approximately 90 seconds. The analysis has shown that vertical thrusters did not supply enough thrust to follow the desired slope towards the target. However, increased drop-outs of the acoustic link were the main reason for inferior tracking performance. Due to prolonged drop-outs (more than 5 s), the UUV safety mechanism was triggered, where the UUV control would shut down all thrusters. Since the UUV is positively buoyant, this explains why vertical tracking behaved worse than horizontal. More effort will be needed to increase the acoustic link reliability and investigate the possible reasons for the drop-outs.

VI. Conclusion

This paper describes results which show potential for collaborative use of autonomous vehicles in MCM and, more generally, aided navigation. The main goal was the employment of an autonomous vehicle to minimize the workload on the operator. The autonomous system prototype is designed to be scalable to the needs of the operation, and to offer an increase in the tempo of operations.

We mentioned before that range and bearing information need to be transmitted regularly to the UUV. During initial testing a tethered connection was used, both for convenience and safety. This drastically eased data transmission. Tethered communication was reliable and had negligible transmission delay. Both of these are not present when switching to acoustic communication. The reliability issue is tackled by using robust transmission protocols. Transmission delays introduced by the acoustic communications are as high as two seconds. Higher transmission rates are possible but will probably increase vehicle cost. Therefore optimization of the data transfer with the existing modem will be researched.

Future work will include research on sonar image processing and implementation of estimators which compensate for the delays in measurements emitted via acoustic link. Implementation of the whole concept and testing in real-life conditions will be undertaken. Additional methods of signature association will be researched. This is needed to accurately recognize false readings so that the mission can be paused when the vehicle is lost from the sonar image.

VII. Acknowledgments

The success of the experiments reported in this article owes great credit to the computer programmers, engineering team, and technicians who integrated new functionality into the vehicles and kept them operational in sometimes difficult operating environments, especially Dr. Stefano Fioravanti, Arjan Vermeij and Alberto Grati. Part of the work was performed under the NATO Undersea Research Centre Consolidated Programme of Work. The work was also carried out in the framework of a Coordination and Support Action type of project supported by the European Commission under the Seventh Framework Programme "CURE – Developing Croatian Underwater Robotics Research Potential" SP-4 Capacities (call FP7–REGPOT–2008–1) under Grant Agreement Number: 229553.

References

[1] A. Alcocer, P. Oliveira, and A. Pascoal. Study and implementation of an EKF GIB-based underwater positioning system. In *IFAC CAMS04*, 2004.

[2] F. Baralli, B. Evans, E. Coiras, and A. Bellettini. AUV navigation for MCM operations. Technical report, NATO Undersea Research Centre, La Spezia, Italy, 2007.

[3] M. Caccia, G. Indiveri, and G. Veruggio. Modelling and identification of open-frame variable configuration unmanned underwater vehicles. *IEEE Journal of Oceanic Engineering*, 25(2):227–240, 2000.

[4] D. Clark, I.T. Ruiz, Y. Petillot, and J. Bell. Particle phd filter multiple target tracking in sonar image. *Aerospace and Electronic Systems, IEEE Transactions on*, 43(1):409 –416, 2007.

[5] H.J.S. Feder, J.J. Leonard, and C.M. Smith. Adaptive sensing for terrain aided navigation. In *OCEANS '98 Conference Proceedings*, volume 1, pages 336–341, 1998.

[6] H. Johannsson, M. Kaess, B. Englot, F. Hover, and J. Leonard. Imaging sonar-aided navigation for autonomous underwater harbor surveillance. In *Intelligent Robots and Systems (IROS), 2010 IEEE/RSJ International Conference on*, pages 4396 –4403, 2010.

[7] J. C. Kinsey, R. M. Eustice, and L. L. Whitcomb. A survey of underwater vehicle navigation: recent advances and new challenges. In *procedings of 7th IFAC Conference on Manoeuvring and Control of Marine Craft*, 2006.

[8] T. Kirubarajan and Y. Bar-Shalom. Probabilistic data association techniques for target tracking in clutter. *Proceedings of the IEEE*, 92(3):536 – 557, 2004.

[9] Martin E. Liggins, David L. Hall, and James Llinas. *Handbook of Multisensor Data Fusion*. CRC Press, 2009.

[10] P.A. Miller, J.A. Farrell, Yuanyuan Zhao, and V. Djapic. Autonomous underwater vehicle navigation. *IEEE Journal of Ocean Engineering*, 35(3):663 – 678, 2010.

[11] N. Miskovic, Z. Vukic, M. Bibuli, G. Bruzzone, and M. Caccia. Fast in-field identification of unmanned marine vehicles. *Journal of Field Robotics*, 28(1):101–120, 2011. doi: 10.1002/rob.20374.

[12] N. Mišković, Đ. Nađ, and Z. Vukić. 3D line following for unmanned underwater vehicles. *Brodogradnja : časopis brodogradnje i brodograđevne industrije*, 61(2):121–129, April 2010.

[13] P. Newman and H. F. Durrant-Whyte. Toward terrain-aided navigation of a subsea vehicle. In *FSR '97 International Conference on Field and Service Robotics*, volume 1, pages 244–248, 1997.